

Catalytic Formation of C(sp³)–F Bonds via Heterogeneous Photocatalysis

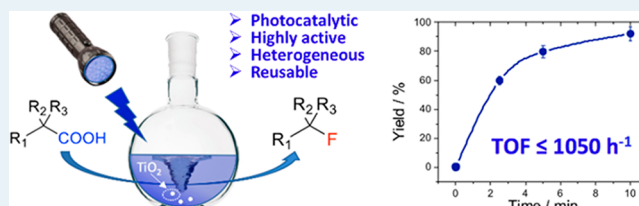
Giulia Tarantino[†] and Ceri Hammond^{*†}

[†]Cardiff Catalysis Institute, Cardiff University, Park Place, Cardiff CF10 3AT, U.K.

Supporting Information

ABSTRACT: Due to their chemical, physical, and biological properties, fluorinated compounds are widely employed throughout society. Yet, despite their critical importance, current methods of introducing fluorine into compounds suffer from severe drawbacks. For example, several methods are noncatalytic and employ stoichiometric equivalents of heavy metals. Existing catalytic methods, on the other hand, exhibit poor activity, generality, selectivity and/or have not been achieved by heterogeneous catalysis, despite the many advantages such an approach would provide. Here, we demonstrate how selective C(sp³)–F bond synthesis can be achieved via heterogeneous photocatalysis. Employing TiO₂ as photocatalyst and Selectfluor as mild fluorine donor, effective decarboxylative fluorination of a variety of carboxylic acids can be achieved in very short reaction times. In addition to displaying the highest turnover frequencies of any reported fluorination catalyst to date (up to 1050 h⁻¹), TiO₂ also demonstrates excellent levels of durability, and the system is catalytic in the number of photons required; i.e., a photon efficiency greater than 1 is observed. These factors, coupled with the generality and mild nature of the reaction system, represent a breakthrough toward the sustainable synthesis of fluorinated compounds.

KEYWORDS: fluorination, photochemistry, heterogeneous catalysis, spectroscopy, photocatalysis



INTRODUCTION

Increasing demand for fluorinated compounds, widely employed as pharmaceuticals, agrochemicals, materials,¹ or tracers for positron emission tomography (as ¹⁸F),² has prompted a surge of interest in the development of new strategies to perform selective fluorination. However, while many breakthroughs have been made,³ such as the development of safer electrophilic fluorinating agents such as Selectfluor, the selective and catalytic formation of C(sp³)–F bonds remains an immense challenge. Indeed, catalytic methods for C(sp³)–F bond formation are rare, and even when catalysis is achieved, other issues such as poor activity, low selectivity, and/or factors associated with scalability—particularly recovery and reuse of the catalyst—are prevalent.

Among various enabling technologies,⁴ recent studies have demonstrated the potential of using light to facilitate fluorination chemistry, with Selectfluor as fluorinating agent and homogeneous species as photocatalysts.⁵ Combining fluorination with photocatalysis (photofluorination) represents a very powerful and sustainable approach and represents a major breakthrough for the field. However, several disadvantages are observed with these previous methods. For example, the reaction mechanisms predominating during such processes have not yet been clearly identified, prohibiting detailed structure–function relationships from guiding catalyst design. More critically, the photocatalysts developed to date also suffer from severe drawbacks, including the requirement for high loadings of scarcely available and/or prohibitively expensive metal centers (Ir, Ru), poor levels of intrinsic activity, and/or

difficulties associated with their molecular complexity and homogeneous nature (recovery, reusability, scalability).⁵ Herein, we demonstrate that commercially available titanium dioxide, TiO₂, a nontoxic, stable, and readily available semiconductor, can be efficiently employed as a heterogeneous photofluorination catalyst. When combined with the decarboxylative fluorination reaction—a powerful and sustainable method for C(sp³)–F bond synthesis⁶—selective photofluorination of a variety of aliphatic carboxylic acids can be achieved under mild electrophilic fluorinating conditions. Under 365 nm irradiation, remarkable fluorine yields can be achieved in very short reaction times (<10 min), resulting in turnover frequency (TOF) values over 1 order of magnitude larger than previously reported (1050 h⁻¹).⁵ The employment of water as solvent, the avoidance of precious metals, and the facile recovery of TiO₂—reusable up to four times—also dramatically increase the sustainability of this method over alternative fluorination methods. Spectroscopic studies with diffuse reflectance infrared Fourier transform (DRIFT) spectroscopy, temperature-programmed desorption mass spectrometry (TPD-MS), ¹⁹F magic angle spinning (MAS) NMR, and X-ray photoelectron spectroscopy (XPS) are coupled to classical mechanistic studies and actinometry, allowing a preliminary reaction mechanism, in which a combination of

Received: July 19, 2018

Revised: September 17, 2018

Published: September 20, 2018

Scheme 1. Photocatalytic Decarboxylative Fluorination of 2,2-Dimethylglutaric Acid (DMGA, 1a) To Yield 4-Fluoro-4-methylpentanoic Acid (4F4MPA, 1b)

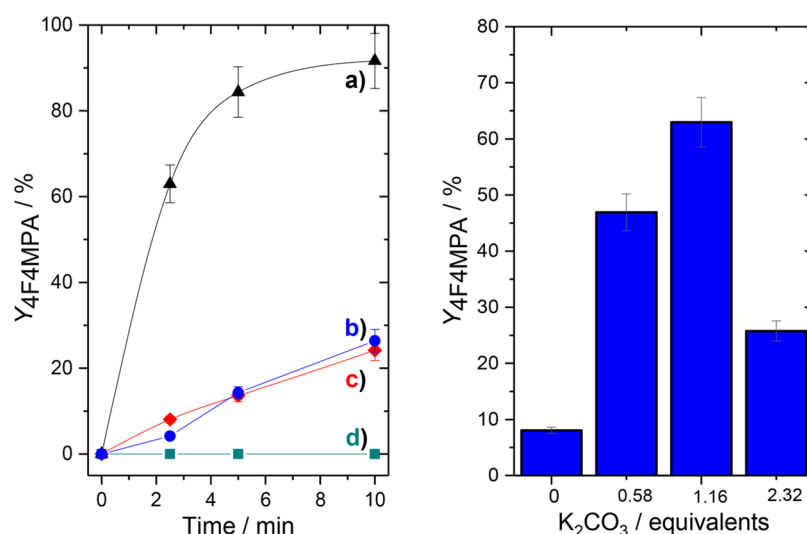
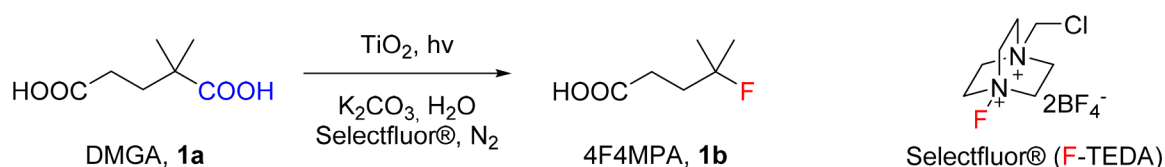


Figure 1. (Left). Yield of 4F4MPA (**1b**) with time over TiO₂ (P25) (a) under standard conditions, (b) in the absence of TiO₂, (c) in the absence of K₂CO₃, and (d) in the absence of Selectfluor. (Right). Yield of 4F4MPA (**1b**) at 2.5 min with various amounts of K₂CO₃ over TiO₂(P25). Standard reaction conditions: 0.2 mmol of DMGA (**1a**), 0.4 mmol of Selectfluor, 0.0125 mmol of TiO₂, 4 mL of H₂O, 0.23 mmol of K₂CO₃, N₂ atmosphere, 25 °C. Solar light simulator (300 W Xe arc lamp) was used to irradiate the reaction mixture.

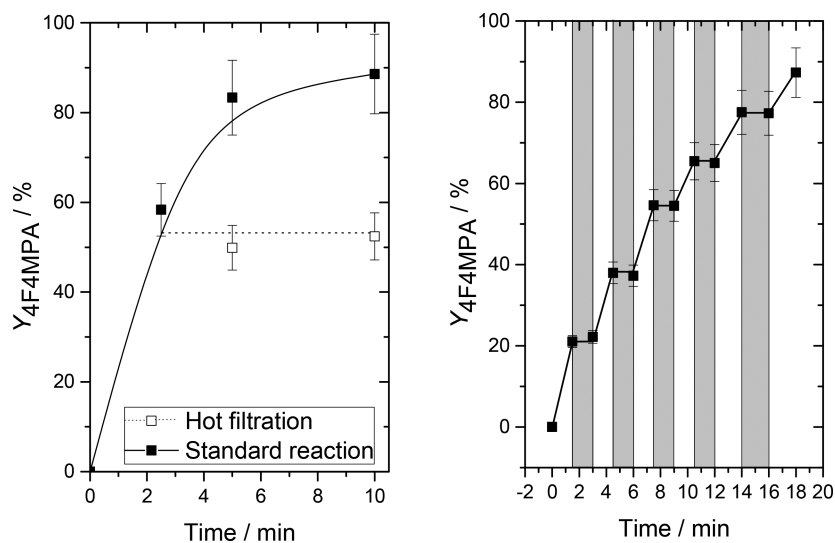


Figure 2. (Left) Solid line: yield of 4F4MPA (**1b**) with time without filtering the catalyst. Dashed line: catalytic activity of the supernatant solution following filtration of the catalyst at 2.5 min. (Right) Yield of 4F4MPA (**1b**) with time over TiO₂ in light and dark (gray area) conditions. Reaction conditions: 1.0 mmol of DMGA (**1a**), 2.0 mmol of Selectfluor, 0.0125 mmol of TiO₂, 10 mL of H₂O, 1.16 mmol of K₂CO₃, N₂ atmosphere, 25 °C. Solar light simulator (300 W Xe arc lamp) was used to irradiate the reaction mixture.

TiO₂-catalyzed steps and free-radical process combine, to be proposed.

RESULTS AND DISCUSSION

Photocatalytic Fluorination. Among a range of well-known photosensitive materials, we identified that commercially available TiO₂ (P25) possessed high levels of activity for

the decarboxylative fluorination of aliphatic carboxylic acids, such as 2,2-dimethylglutaric acid (DMGA, **1a**). Under classical decarboxylative conditions (25 °C, Selectfluor, aqueous phase, SI section 1, Scheme 1),⁶ rapid fluorination of water-soluble acids could be achieved when TiO₂ was irradiated by a solar light simulator or a 365 nm LED torch. Under irradiation, selective monofluorination of DMGA to 4-fluoro-4 methyl-

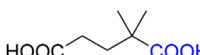
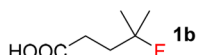
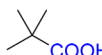
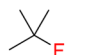
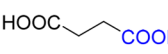
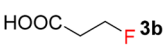
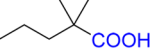

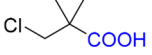
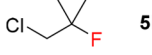
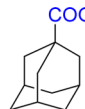
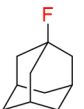
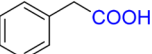
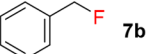
pentanoic acid (4F4MPA, **1b**) was observed, in line with the radical-based mechanism recently reported for this reaction, for which tertiary positions exhibit much higher activity than primary and secondary ones.⁶ Rapid reaction rates were observed, with around 80% 4F4MPA yield achieved in only 5 min of reaction time, when 6.25 mol % of Ti, relative to the substrate, was employed (triangles, Figure 1 (left)). Control reactions were also performed in the absence of K₂CO₃, TiO₂, and Selectfluor. In the absence of the fluorinating agent, no 4F4MPA was observed. Furthermore, in the absence of TiO₂ or K₂CO₃, much lower levels of activity were observed. These indicate the crucial role(s) played by the solid catalyst, the fluorine source, and the base in the reaction network. To further study the effect of base, a number of kinetic experiments at different base loading were performed. Higher activity was observed at 1.16 equiv of K₂CO₃ relative to DMGA (Figure 1 (right)). Interestingly, with a higher amount of base (2.32 equiv), a decrease of reaction rate was observed. Notably, 4F4MPA selectivity >95% was observed in all reactions.

To further optimize the reaction conditions, a number of experiments were performed under more challenging conditions. Excellent performance was still observed at 1.25 mol % of Ti, with a 5-fold decrease in catalyst concentration (Figure 2 (left)) resulting in TOF values of 1050 ± 70 h⁻¹ being observed. Such values are an order of magnitude larger than those reported for any other photofluorination catalyst to date.^{5b} To ensure that the reaction is catalyzed heterogeneously, a hot filtration test was performed (SI section 2). As can be seen (Figure 2 (left)), removing TiO₂ at 2.5 min terminates the reaction, demonstrating catalysis to be heterogeneous. To verify the photocatalytic nature of the reaction, a light/dark experiment was performed by periodically switching the lamp on and off (Figure 2 (right)). Notably, no 4F4MPA formation occurred in the absence of light, confirming that constant irradiation is required for activity to be achieved.

The general applicability of TiO₂ to photofluorinate carboxylic acids was also explored (Table 1, SI Appendix). Interestingly, TiO₂ was also found to be able to photofluorinate primary carboxylic acids, such as succinic acid, **3a**, and 2-phenylacetic acid, **7a**, albeit at lower levels of activity due to the greater difficulty of forming primary alkyl radicals.⁷ Notably, TiO₂ was also able to photofluorinate non-water-soluble substrates when a mixture of water/acetone was used as solvent.

One of the major advantages of heterogeneous catalysts over their homogeneous analogues is the ease in which they can be recovered and reused, leading to increases in process sustainability and scalability. Thus, the durability of TiO₂ to be used in successive cycles was also investigated, using DMGA as substrate and neat water as reaction solvent (Figure 3 (left), SI section 3). Notably, the same final yield values were achieved after 10 min in every catalytic cycle for both fresh and used catalyst. Although a decrease in reaction rate was observed following the first reuse of TiO₂ (Figure S1), no further decrease in performance over successive cycles occurred; i.e., the same kinetic performance was observed for the second, third, and fourth cycles. The ability to reuse the catalyst, without loss in maximum activity over extended cycles, even in the absence of periodic regeneration treatments, is notable and indicates the material possesses potential for extended operation.⁸ Preliminary characterization of fresh and

Table 1. General Applicability of TiO₂ for the Photocatalytic Fluorination of Various Carboxylic Acids

Entry	Substrate	Product	Yield / % ^a
1	 1a	 1b	92, 35 ^b
2	 2a	 2b	94 ^c
3	 3a	 3b	48 ^d
4	 4a	 4b	42 ^e
5	 5a	 5b	46 ^{d,e}
6	 6a	 6b	22 ^e
7	 7a	 7b	17 ^{e,f}

^aYields calculated as “mol (product)/mol (mol substrate) × 100” for entries 1 and 3–7 and as “mol (2a converted)/mol(initial mol 2a)” for entry 2 due to high product volatility. ^b2 mL of H₂O and 2 mL of (CH₃)₂CO as solvent. ^c0.115 mmol of K₂CO₃. ^dReaction time 30 min. ^e5 mL of H₂O, 5 mL of (CH₃)₂CO, 0.115 mmol of K₂CO₃. ^fReaction time: 60 min. Yields calculated with ¹⁹F NMR using α,α,α -trifluorotoluene and HPLC analysis against authentic standards. Reaction conditions: 0.2 mmol of substrate, 0.4 mmol of Selectfluor, 0.0125 mmol of TiO₂, 4 mL of H₂O, 0.23 mmol of K₂CO₃, 25 °C, 10 min. Monochromatic LED irradiation of 365 nm was employed.

used catalyst indicates that although no change in surface area occurs during reaction (55 m² g⁻¹ for both fresh and used sample, Table S1), conversion between the two crystalline phases present in P25, i.e., anatase and rutile, occurs to some extent (Table S2). The relative ratio anatase/rutile was found to decrease slightly following each catalytic cycle, going from a maximum of 86:14 for fresh TiO₂ to a ratio of 78:22, observed at the fourth catalytic cycle. The small phase transformations observed, may, therefore, account for the slight decrease in intrinsic kinetic activity.

To further investigate this, the photocatalytic activity of the two pure crystalline phases, i.e., anatase and rutile, was investigated under the conditions previously employed for P25 using a monochromatic LED torch at 365 nm (Figure 3 (right)). As can be seen, lower levels of performance were exhibited by both pure rutile and pure anatase when compared to P25, in line with previous studies.⁹ Although this may arise from reported synergistic effects, we stress that the poorer performance of both pure phases may also be related to their different physical properties, such as surface area and crystallite size (Figures S2 and S3 and Tables S1–S3).⁹ Notably, different activity was also observed between anatase and rutile, with the latter being less active. However, the higher levels of

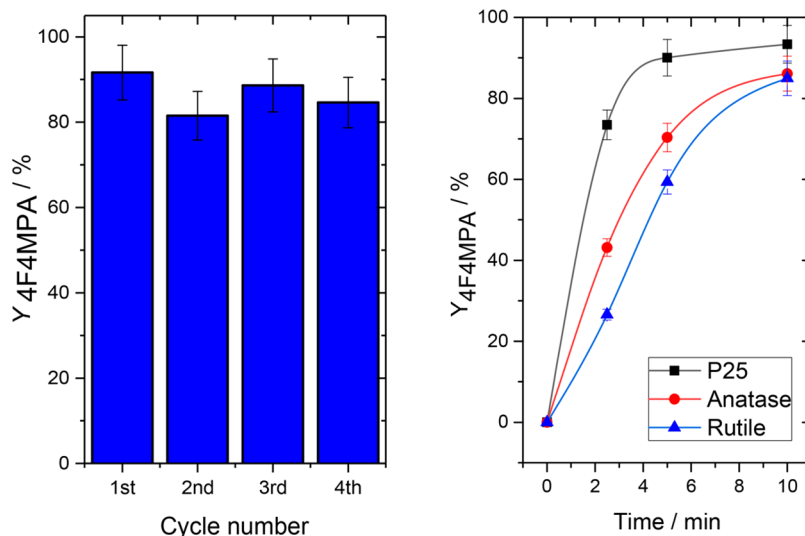


Figure 3. (Left) Reusability of TiO₂ with DMGA (1a) as substrate. No intermediate treatments were performed between cycles. Reaction conditions otherwise identical to Figure 1. (Right) Yield of 4F4MPA (1b) with time over (a) P25, (b) anatase, and (c) rutile. Reaction conditions: 0.2 mmol of DMGA (1a), 0.4 mmol of Selectfluor, 0.0125 mmol of TiO₂, 4 mL of H₂O, 0.23 mmol of K₂CO₃, N₂ atmosphere, 25 °C. Forensic monochromatic LED torch at 365 nm wavelength (Labino Torch Light UVG2 spotlight) was used to irradiate the reaction mixture.

photocatalytic performance exhibited by anatase compared to rutile are in good agreement with several previous reports.¹⁰

Mechanistic Studies. Several potential chemical reactions can occur during photofluorination. Accordingly, obtaining a detailed understanding of the reaction mechanism(s) is extremely challenging. Indeed, from the literature a number of possible reaction mechanisms can be proposed, ranging from SET processes between carboxylate groups bound on TiO₂¹¹ to SET processes between radical alkyl species and Selectfluor.¹² In addition, direct interactions between Selectfluor and TiO₂ could result in formation of Ti–F intermediates,¹³ which may participate in the reaction mechanism. Thus, to gain preliminary insight into the potential mechanism, a variety of spectroscopic experiments were performed.

To investigate the interaction between the substrate and the catalyst, DRIFT studies were performed. These studies were performed on pivalic acid (2a, Table 1), a more volatile substrate than DMGA that also undergoes decarboxylative photofluorination (Table 1). To first establish the nature of the interaction between pivalic acid/TiO₂ in the absence of light, pivalic acid was adsorbed on TiO₂ at 30 °C (Figure 4), and the sample was subsequently heated to 600 °C (Figure 5). After the adsorbate was dosed at 30 °C, new features appeared in the IR spectrum ((i) blue line, Figure 4); a group of bands in the region 3000–2850 cm⁻¹ characteristic of aliphatic C–H stretching, and other signals in the region 1700–1100 cm⁻¹. Interestingly, although the new C–H stretching bands correspond well to those observed for free, i.e., nonadsorbed, pivalic acid ((ii) red line, Figure 4), the signal at 1692 cm⁻¹, characteristic of the key –COOH group ((ii) red line, Figure 4), only appears in low intensity, clearly demonstrating that only a negligible percentage of pivalic acid adsorbs onto the catalyst surface in its free acidic form. However, new vibrations in the region 1600–1100 cm⁻¹ are observed, consistent with those reported for deprotonated pivalic acid, (CH₃)₃CCOO⁻.¹⁴

The thermal stability of the adsorbed pivalic acid was subsequently explored by heating the DRIFT cell to various

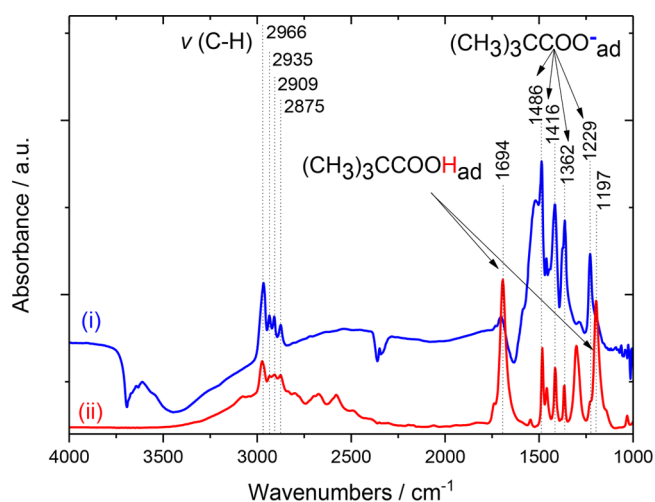


Figure 4. (i) DRIFT spectrum of TiO₂ after adsorption of pivalic acid (blue line) and (ii) DRIFT spectrum of free pivalic acid (red line).

temperatures (Figure 5). While the residual feature at 1692 cm⁻¹ disappears above 50 °C, indicating that the small quantities of pivalic acid in its acid form are merely physisorbed, the vibrations at 1600–1100 cm⁻¹ and the C–H stretching features at 3000–2850 cm⁻¹ are stable during heat treatment. Indeed, all these peaks are still clearly visible at 300–450 °C, temperatures much higher than the boiling point of pivalic acid (165 °C). Therefore, all the new features observed following interaction with TiO₂ can be assigned to a strongly chemisorbed (CH₃)₃CCOO⁻ species (henceforth denoted as (RCOO⁻)_{ads}), indicating the formation of an (RCOO⁻)TiO₂ intermediate.

To evaluate the role of light during the reaction, and to verify the changes observed to the chemisorbed (RCOO⁻)TiO₂ intermediate during photoirradiation, an experiment was performed whereby the DRIFT cell containing the TiO₂-bound carboxylate species was irradiated with a monochromatic light of 365 nm wavelength. Prior to irradiation, no decrease of the intensity of this species was observed over

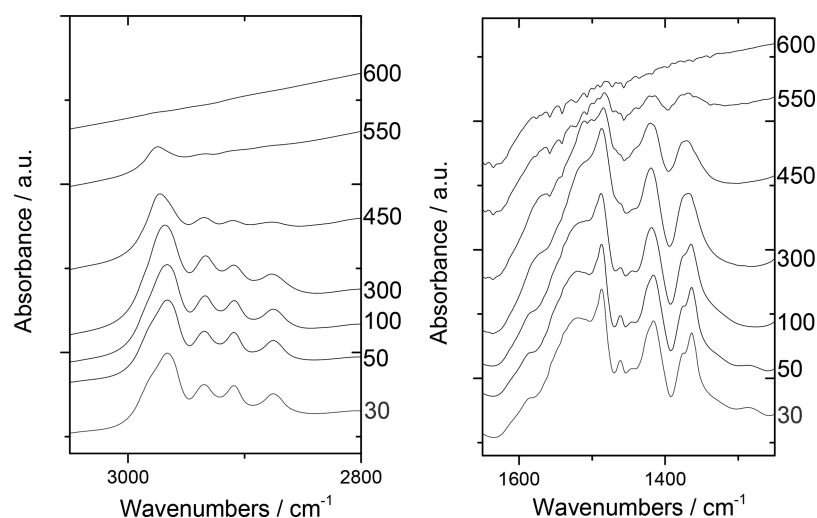


Figure 5. Spectral changes observed to DRIFT spectra of TiO_2 after adsorption of pivalic acid at different temperatures, from 30 °C (bottom line) to 600 °C (top line).

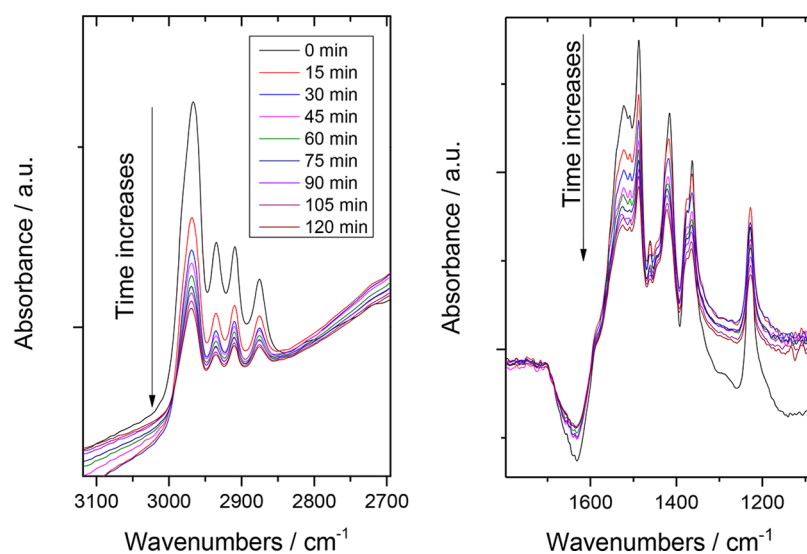


Figure 6. DRIFT spectra of TiO_2 -bound pivalate species during irradiation with a monochromatic UV light of 365 nm (Labino Torch Light UVG2 spotlight).

several hours (Figure S4). Figure 6 presents the spectral changes that occur throughout the irradiation period. Upon irradiation, a continuous decrease of intensity for all the features related to the $(\text{RCOO}^-)\text{TiO}_2$ intermediate was observed. This clearly indicates that pivalate decomposition occurs during the entire irradiation period. Loss of the pivalate under these conditions likely results from its decomposition from RCOO^- into R^\bullet and CO_2 , as reported by Henderson et al. and Manley et al. for classical decarboxylative reactions.¹¹ Further evidence of this mechanism was obtained through the observation of CO_2 in the effluent of a TPD-MS experiment, following photoirradiation of DMGA-treated TiO_2 (Figures S5–9). Accordingly, DRIFTS and TPD-MS studies indicate that the carboxylic acid groups of the substrate bind to the TiO_2 surface in their carboxylate form and only decompose from the surface under photoirradiation, accompanied by the loss of CO_2 .^{11,14}

In addition to substrate/ TiO_2 interactions, the contribution of potential F/ TiO_2 intermediates was also evaluated. Indeed, fluorination of TiO_2 surfaces, resulting in the formation of

various Ti–F species, has been widely reported.¹³ To investigate the potential involvement of such species in the reaction mechanism, 300 mg of TiO_2 was treated with an aqueous solution of Selectfluor under general reaction conditions, but in the absence of the substrate. Analysis of this sample by XPS revealed that, following treatment, residual amounts of fluorine species (0.08 mmol g^{-1}) with a binding energy of 684.6 eV were found on the catalyst surface (Figures S10–14). ^{19}F MAS NMR analysis of the same sample (Figures S15 and S16) indicates the covalent nature of this interaction (henceforth denoted as F/ TiO_2), in line with the previous report of Dambournet.¹⁵ Notably, these species were also observed on used catalysts (Figure S10 and Table S4).

To investigate the potential role of F/ TiO_2 , isolated samples containing this species were screened for reactivity by performing the photofluorination of DMGA in the absence of other fluorinating agents but with F/ TiO_2 present as catalyst. Although the catalyst containing a sufficient amount of fluorine permitted up to 80% yield to be achieved, no conversion and no 4F4MPA yield were detected under the

standard photofluorination conditions over a period of 30 min. This excludes the possibility of F/TiO₂ species acting as the active fluorinating species and suggests that Selectfluor containing active fluorine (F-TEDA, Figure 7) is directly

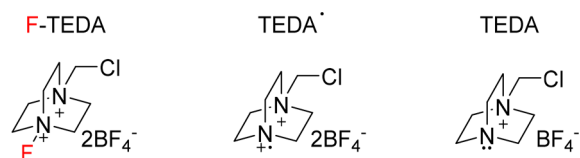


Figure 7. Schematic representation of F-TEDA and its subsequent decomposition products.

responsible for fluorine transfer. To allow proper discrimination among F-TEDA and its decomposition products, the notations displayed in Figure 7 are adopted in the sections below.

Following identification of F-TEDA as the active fluorine-transfer agent, the stoichiometry of the decarboxylative fluorination reaction, in terms of F-TEDA consumed to 4F4MPA produced, was explored, by decreasing the amount of Selectfluor from the 2 equiv typically used under standard conditions to 1 and 0.5 equiv, respectively. When 1 and 0.5 equiv were employed for DMGA decarboxylative fluorination, 4F4MPA yields up to 84% and 41% were achieved, respectively (Figure 8 (left)). To better understand the stoichiometry, F-TEDA consumption was also measured at different reaction times via ¹⁹F NMR by monitoring the disappearance of signal at $\delta = +48$ ppm (characteristic to the N–F bond) (Figure S17). This analysis confirmed that 1.2 equiv are required for 1 equiv of 4F4MPA to be produced at the lowest F-TEDA concentrations (Tables S5 and S6). Notably, the initial reaction rate (*k*) measured at different starting concentrations of F-TEDA also demonstrated a linear dependence on the initial concentration of F-TEDA (Figures S18 and S19), indicating that F-TEDA is involved in the rate-determining step of the reaction. However, the small excess of F-TEDA

required (1.2 equiv) also indicates that competitive reaction pathways, leading to passivation of F-TEDA, occur. This is in line with our previous findings (vide supra), involving the formation of inactive F/TiO₂ species, as observed by both XPS and ¹⁹F MAS NMR.

The consumption of F-TEDA may occur from several processes, such as (i) general instability under the aqueous environment, (ii) selective consumption as a consequence of reaction, i.e., following attack by the alkyl radical R[•], (iii) nonselective interactions with the base, and (iv) nonselective interactions with TiO₂, i.e., F/TiO₂ formation. In order to investigate the extent of these pathways, the amount of F-TEDA converted at 10 min was monitored under otherwise-standard reaction reactions, but (i) in the absence of TiO₂, (ii) in the absence of K₂CO₃, and (iii) in the absence of the substrate, DMGA (1a) (Figure 8 (right)). Interestingly, complete conversion of F-TEDA was observed even in the absence of the substrate, when both TiO₂ and K₂CO₃ were present, indicating that F-TEDA can be converted even in the absence of substrate. However, in the absence of either TiO₂ or K₂CO₃, much lower levels of F-TEDA were converted. In addition to confirming the essential role of TiO₂ in catalyzing all stages of the reaction, this observation suggests that in addition to being required to deprotonate the substrate, favoring the formation of the (R-COO⁻)TiO₂ intermediate, an additional role of K₂CO₃ in the reaction mechanism may be to act as a sacrificial electron donor (i.e., hole scavenger), favoring charge separation e⁻/h⁺ in photoactivated TiO₂.¹⁶ This may account for the observation that the optimal amount of K₂CO₃ is just over 1 equiv, relative to DMGA (Figure 1 (right)). In the absence of substrate, TiO₂ and K₂CO₃, no F-TEDA was consumed, pointing to its otherwise stable nature under the general reaction conditions. Additional experiments performed replacing K₂CO₃ with a strong Brønsted–Lowry base, NaOH (Figure S20), indicate that, although good catalytic performances are still observed in the presence of NaOH, higher catalytic activity is achieved in the presence of K₂CO₃. This

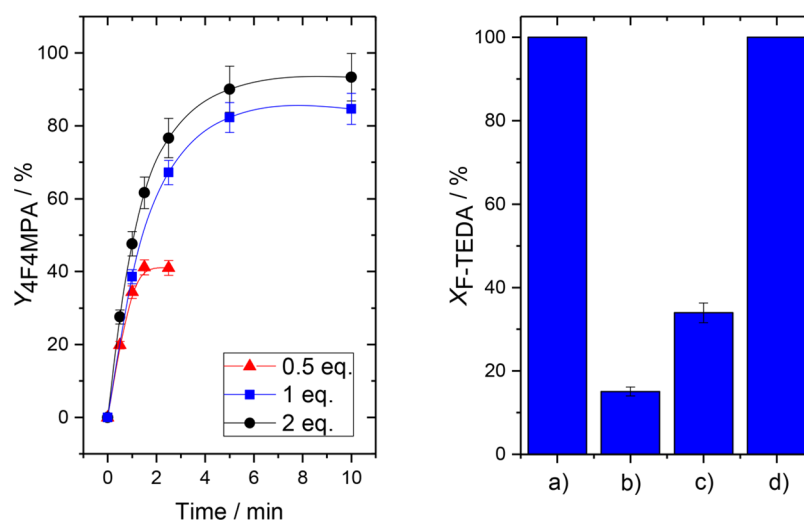
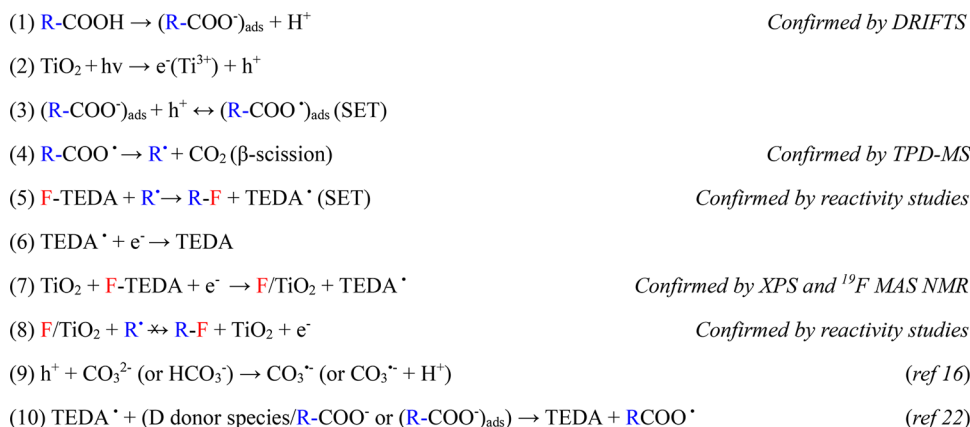


Figure 8. (Left) Yield of 4F4MPA (1b) with time over TiO₂ with (i) 0.5 equiv of Selectfluor, 0.1 mmol (triangle), (ii) 1 equiv of Selectfluor, 0.2 mmol (squares), and (iii) 2 equiv of Selectfluor, 0.4 mmol (circles). Reaction conditions: 0.2 mmol of DMGA (1a), various amounts of Selectfluor, 0.0125 mmol of TiO₂, 4 mL of H₂O, 0.23 mmol of K₂CO₃, 25 °C, N₂. Forensic monochromatic LED torch at 365 nm wavelength (Labino Torch Light UVG2 spotlight) was used to irradiate the reaction mixture. (Right) Conversion of F-TEDA at 10 min (a) under standard conditions, (b) under standard conditions but without TiO₂, (c) under standard conditions but without K₂CO₃, and (d) under standard conditions but without DMGA (1a).

Scheme 2. Overall Reaction Mechanism



may be due to the ability of the carbonate species to consume the photogenerated holes (h^+), forming carbonate radicals.

Considering the radical nature of several species involved in the reaction mechanism, the effect of O_2 , a well-known alkyl radical scavenger, was also investigated.¹⁷ Performing the reaction in O_2 , as opposed to N_2 , resulted in a decrease in 4F4MPA yield (Figure S21). The decrease in 4F4MPA in the presence of O_2 implies that alkyl radicals may be involved in the rate-determining step. This is in line with the known ability of O_2 to trap carbon-centered radicals, hence prohibiting the introduction of fluorine.¹⁷

Identifying the Photocatalytic Properties of the System. In photocatalysis, the number of photons efficiently employed in a chemical process is one of the key parameters to describe the efficiency of the system, allowing proper comparison with other existing photocatalytic systems. Therefore, the apparent number of photons efficiently employed (“apparent photon efficiency, ξ ”) for decarboxylative fluorination under reaction conditions was measured by calculating the ratio between the number of molecules converted over time versus the number of incident photons under the same period of time. It is noteworthy to mention that in heterogeneous catalysis it is important to discriminate between the number of incident photons and the number of photons efficiently absorbed by the solid catalyst and the term quantum yield, Φ (or quantum efficiency), can be correctly employed only as a function of the number of photons actually absorbed by the catalyst.¹⁸

$$\xi = \frac{\text{molecules of substrate converted}}{\text{no. of incident photons}}$$

$$\Phi = \frac{\text{molecules of substrate converted}}{\text{no. of absorbed photons}}$$

Considering that the number of incident photons is always higher than the number of photons absorbed by the heterogeneous material, ξ is always lower than the quantum yield, Φ , of the system. However, ξ may still be used to investigate if light behaves as a true catalyst (ξ greater than 1) or not (photosensitized process), even though it does not give real information on the quantum yield of the system. To investigate the catalytic properties of light in the system, the photon flow through the aqueous reaction mixture was determined using a standard ferrioxalate actinometry method¹⁹ under 365 nm light irradiation (Figures S22 and S23). Under these conditions, a photon flow of $(2.0 \pm 0.5) \times 10^{17}$ photons/s was measured. This value was then used to measure the

“apparent photon efficiency” of the system as a ratio between the number of molecules of DMGA converted (at 30 and 60 s) and the number of incident photons (photon flow \times 30 and 60 s, respectively), giving an “apparent photon efficiency” of 3.5 ± 0.5 . An apparent photon efficiency greater than 1 implies an even higher quantum efficiency of the system, thus indicating that light is a true catalyst for this reaction, with one absorbed photon being able to catalyze more than one catalytic cycle. This further suggests that a free-radical chain mechanism dominates, contributing to the overall reaction mechanism, although light and TiO_2 are both essential for the catalytic activity to be observed. Preliminary investigation into the effect of the intensity of the light on the reaction rate was also performed, showing correlation between the intensity of the light source and the reaction rate (Figure S24). The observation of the catalytic nature of light in the system further demonstrates the high levels of sustainability exhibited by this system, relative to classical methods of fluorination.

Overall Reaction Mechanism. Based on all the observations described above, an overall reaction mechanism can be proposed (Scheme 2).

DRIFT analysis indicates that carboxylic acids bind to the TiO_2 surface in their carboxylate form (1).¹⁴ This may account for the poor catalytic performances observed exhibited by TiO_2 when K_2CO_3 is not present in the reaction mixture. Simultaneous to substrate adsorption, photoexcitation of TiO_2 with UV light leads to the formation of electron–hole pairs (2). The positive holes (h^+) so generated can subsequently withdraw an electron from the chemisorbed carboxylate species according to the photo-Kolbe reaction²⁰ via SET, leading to the generation of radical species R-COO^{\bullet} (3). These radicals can then decompose (β -scission) to yield CO_2 (observed by TPD-MS in the absence of Selectfluor) and alkyl radical species R^{\bullet} (4). The presence of R^{\bullet} is inferred from the radical nature of the reaction (apparent photon efficiency greater than 1) and the negative role exhibited by O_2 in the system.¹⁷ Alternatively, R-COO^{\bullet} species can also further react with TiO_2 via additional SET, re-establishing the R-COO^{\bullet} species. Since it is known that F-TEDA ($E^0 = -0.296$ V vs Ag/Ag^+ electrode)²¹ is able to functionalize such radical substrates through SET, we hypothesize that following decarboxylation, the alkyl radical species, R^{\bullet} , reacts with F-TEDA, resulting in the formation of the desired R-F product, and an equivalent of the radical TEDA^{\bullet} (5). Notably, the radical species TEDA^{\bullet} can subsequently trap the free electron released by photoexcitation of TiO_2 , resulting in the more stable species TEDA ,

- 37, 308–319. (c) Liang, T.; Neumann, C. N.; Ritter, T. Introduction of Fluorine and Fluorine-Containing Functional Groups. *Angew. Chem., Int. Ed.* **2013**, *52*, 8214–8264. (d) Purser, S.; Moore, P. R.; Swallow, S.; Gouverneur, V. Fluorine in Medicinal Chemistry. *Chem. Soc. Rev.* **2008**, *37*, 320–330. (e) Ritter, T. Catalysis: Fluorination Made Easier. *Nature* **2010**, *466*, 447–448.
- (2) (a) Miller, P. W.; Long, N. J.; Vilar, R.; Gee, A. D. Synthesis of ^{11}C , ^{18}F , ^{15}O and ^{13}N Radiolabels for Positron Emission Tomography. *Angew. Chem., Int. Ed.* **2008**, *47*, 8998–9033. (b) Littich, R.; Scott, P. J. H. Novel Strategies for Fluorine-18 Radiochemistry. *Angew. Chem., Int. Ed.* **2012**, *51*, 1106–1109. (c) Brooks, A. F.; Topczewski, J. J.; Ichishi, N.; Sanford, M. S.; Scott, P. J. H. Late-stage [^{18}F] Fluorination: New Solutions to Old Problems. *Chem. Sci.* **2014**, *5*, 4545–4553.
- (3) (a) Liu, W.; Huang, X.; Cheng, M. J.; Nielsen, R. J.; Goddard, W. A., III; Groves, J. T. Oxidative Aliphatic C-H Fluorination with Fluoride Ion Catalyzed by a Manganese Porphyrin. *Science* **2012**, *337*, 1322–1325. (b) Sibi, M. P.; Landais, Y. C(sp 3)-F Bond Formation: a Free-Radical Approach. *Angew. Chem., Int. Ed.* **2013**, *52*, 3570–3572. (c) Furuya, T.; Kamlet, A. S.; Ritter, T. Catalysis for Fluorination and Trifluoromethylation. *Nature* **2011**, *473*, 470–477. (d) Liu, W.; Groves, J. T. Manganese-Catalyzed Oxidative Benzylic C-H fluorination by Fluoride Ions. *Angew. Chem., Int. Ed.* **2013**, *52*, 6024–6027. (e) Hull, K. L.; Anani, W. Q.; Sanford, M. S. Palladium-Catalyzed Fluorination of Carbon-Hydrogen Bonds. *J. Am. Chem. Soc.* **2006**, *128*, 7134–7135. (f) Watson, D. A.; Su, M.; Teverovskiy, G.; Zhang, Y.; Garcia-Fortanet, J.; Kinzel, T.; Buchwald, S. L. Formation of ArF from LPdAr(F): Catalytic Conversion of Aryl Triflates to Aryl Fluorides. *Science* **2009**, *325*, 1661–1664. (g) Hickman, A. J.; Sanford, M. S. High-Valent Organometallic Copper and Palladium in Catalysis. *Nature* **2012**, *484*, 177–185.
- (4) (a) Howard, J. L.; Sagatov, Y.; Repousseau, L.; Schotten, C.; Browne, D. L. Controlling Reactivity Through Liquid Assisted Grinding: The Curious Case of Mechanochemical Fluorination. *Green Chem.* **2017**, *19*, 2798–2802. (b) Wang, Y.; Wang, H.; Jiang, Y.; Zhang, C.; Shao, J.; Xu, D. Fast, Solvent-Free and Highly Enantioselective Fluorination of β -Keto Esters Catalyzed by Chiral Copper Complexes in a Ball Mill. *Green Chem.* **2017**, *19*, 1674–1677.
- (5) (a) Ventre, S.; Petronijevic, F. R.; MacMillan, D. W. C. Decarboxylative Fluorination of Aliphatic Carboxylic Acids via Photoredox Catalysis. *J. Am. Chem. Soc.* **2015**, *137*, 5654–5657. (b) Porras, J. A.; Mills, I. N.; Transue, W. J.; Bernhard, S. Highly Fluorinated Ir(III)-2,2':6',2''-Terpyridine-Phenylpyridine-X Complexes via Selective C–F Activation: Robust Photocatalysts for Solar Fuel Generation and Photoredox Catalysis. *J. Am. Chem. Soc.* **2016**, *138*, 9460–9472. (c) Rueda-Becerril, M.; Mahé, O.; Drouin, M.; Majewski, M. B.; West, J. G.; Wolf, M. O.; Sammis, G. M.; Paquin, J.-F. Direct C-F Bond Formation Using Photoredox Catalysis. *J. Am. Chem. Soc.* **2014**, *136*, 2637–2641. (d) Kee, C. W.; Chin, K. F.; Wong, M. W.; Tan, C.-H. Selective Fluorination of Alkyl C-H Bonds via Photocatalysis. *Chem. Commun.* **2014**, *50*, 8211–8214. (e) Wu, X.; Meng, C.; Yuan, X.; Jia, X.; Qian, X.; Ye, J. Transition-Metal-Free Visible-Light Photoredox Catalysis at Room Temperature for Decarboxylative Fluorination of Aliphatic Carboxylic Acids by Organic Dyes. *Chem. Commun.* **2015**, *51*, 11864–11867. (f) West, J. G.; Bedell, T. A.; Sorensen, E. J. The Uranyl Cation as a Visible-Light Photocatalyst for C(sp 3)-H Fluorination. *Angew. Chem., Int. Ed.* **2016**, *55*, 8923–8927. (g) Neumann, C. N.; Ritter, T. C-H Fluorination: U Can Fluorinate Unactivated Bonds. *Nat. Chem.* **2016**, *8*, 822–823. (h) Leung, J. C. T.; Chatalova-Sazepin, C.; West, J. G.; Rueda-Becerril, M.; Paquin, J.-F.; Sammis, G. M. Photo-fluorodecarboxylation of 2-Aryloxy and 2-Aryl Carboxylic Acids. *Angew. Chem., Int. Ed.* **2012**, *51*, 10804–10807. (i) Bloom, S.; Pitts, C. R.; Miller, D. C.; Haselton, N.; Holl, M. G.; Urheim, E.; Lectka, T. A Polycyclic Metal-Catalyzed Aliphatic, Allylic, and Benzylic Fluorination. *Angew. Chem., Int. Ed.* **2012**, *51*, 10580–10583. (j) Pitts, C. R.; Bloom, S.; Woltonist, R.; Auvenshine, D. J.; Ryzhkov, L. R.; Siegler, M. A.; Lectka, T. Direct, Catalytic Monofluorination of sp 3 C–H Bonds: A Radical-Based Mechanism with Ionic Selectivity. *J. Am. Chem. Soc.* **2014**, *136*, 9780–9791. (k) Bloom, S.; McCann, M.; Lectka, T. Photocatalyzed Benzylic Fluorination: Shedding “Light” on the Involvement of Electron Transfer. *Org. Lett.* **2014**, *16*, 6338–6341.
- (6) Yin, F.; Wang, Z.; Li, Z.; Li, C. Silver-Catalyzed Decarboxylative Fluorination of Aliphatic Carboxylic Acids in Aqueous Solution. *J. Am. Chem. Soc.* **2012**, *134*, 10401–10404.
- (7) Blanksby, S. J.; Ellison, G. B. Bond Dissociation Energies of Organic Molecules. *Acc. Chem. Res.* **2003**, *36*, 255–263.
- (8) Hammond, C. Intensification studies of Heterogeneous Catalysts: Probing and Overcoming Catalyst Deactivation During Liquid Phase Operation. *Green Chem.* **2017**, *19*, 2711–2728.
- (9) Su, R.; Bechstein, R.; Sø, L.; Vang, R. T.; Sillassen, M.; Esbjörnsson, B.; Palmqvist, A.; Besenbacher, F. How the Anatase-to-Rutile Ratio Influences the Photoreactivity of TiO $_2$. *J. Phys. Chem. C* **2011**, *115*, 24287–24292.
- (10) Luttrell, T.; Halpegamage, S.; Tao, J.; Kramer, A.; Sutter, E.; Batzill, M. Why is Anatase a Better Photocatalyst Than Rutile? – Model Studies on Epitaxial TiO $_2$ Films. *Sci. Rep.* **2015**, *4*, 4043.
- (11) (a) Henderson, M. A.; White, J. M.; Uetsuka, H.; Onishi, H. Photochemical Charge Transfer and Trapping at the Interface Between an Organic Adlayer and an Oxide Semiconductor. *J. Am. Chem. Soc.* **2003**, *125*, 14974–14975. (b) Manley, D. W.; McBurney, R. T.; Miller, P.; Walton, J. C. Titania-Promoted Carboxylic Acid Alkylations of Alkenes and Cascade Addition-Cyclizations. *J. Org. Chem.* **2014**, *79*, 1386–1398.
- (12) Rueda-Becerril, M.; Chatalova Sazepin, C.; Paquin, J.; Sammis, G. Fluorine Transfer to Alkyl Radicals. *J. Am. Chem. Soc.* **2012**, *134*, 4026–4029.
- (13) (a) Sun, H.; Wang, S.; Ang, H. M.; Tadé, M. O.; Li, Q. Halogen Element Modified Titanium Dioxide for Visible Light Photocatalysis. *Chem. Eng. J.* **2010**, *162*, 437–447. (b) Moss, J. H.; Parfitt, G. D.; Fright, A. The Fluorination of Titanium Dioxide Surfaces. *Colloid Polym. Sci.* **1978**, *256*, 1121–1130. (c) Shifu, C.; Yunguang, Y.; Wei, L. Preparation, Characterization and Activity Evaluation of TiN/F-TiO $_2$ Photocatalyst. *J. Hazard. Mater.* **2011**, *186*, 1560–1567.
- (14) (a) Wen, B.; Li, Y.; Chen, C.; Ma, W.; Zhao, J. An Unexplored O $_2$ -Involved Pathway for the Decarboxylation of Saturated Carboxylic Acids by TiO $_2$ Photocatalysis: An Isotopic Probe Study. *Chem. - Eur. J.* **2010**, *16*, 11859–11866. (b) Backes, M. J.; Lukaski, A. C.; Muggli, D. S. Active Sites and Effects of H $_2$ O and Temperature on the Photocatalytic Oxidation of ^{13}C -Acetic Acid on TiO $_2$. *Appl. Catal., B* **2005**, *61*, 21–35. (c) Szabó-Bárdos, E.; Baja, B.; Horváth, E.; Horváth, A. Photocatalytic Decomposition of L-Serine and L-Aspartic Acid Over Bare and Silver-Deposited TiO $_2$. *J. Photochem. Photobiol., A* **2010**, *213*, 37–45.
- (15) (a) Li, W.; Body, M.; Legein, C.; Dambournet, D. Identify OH Groups in TiOF $_2$ and their Impact on the Lithium Intercalation Properties. *J. Solid State Chem.* **2017**, *246*, 113–118. (b) Li, W.; Body, M.; Legein, C.; Borkiewicz, O. J.; Dambournet, D. Atomic Insights into Nanoparticle Formation of Hydroxyfluorinated Anatase Featuring Titanium Vacancies. *Inorg. Chem.* **2016**, *55*, 7182–7187. (c) Li, W.; Body, M.; Legein, C.; Dambournet, D. Sol-Gel Chemistry of Titanium Alkoxide Toward HF: Impacts of Reaction Parameters. *Cryst. Growth Des.* **2016**, *16*, 5441–5447.
- (16) Dimitrijevic, N. M.; Vijayan, B. K.; Poluektov, O. G.; Rajh, T.; Gray, K. A.; He, H.; Zapol, P. Role of Water and Carbonates in Photocatalytic Transformation of CO $_2$ to CH $_4$ on Titania. *J. Am. Chem. Soc.* **2011**, *133*, 3964–3971.
- (17) Maillard, B.; Ingold, K. U.; Scaiano, J. C. Rate Constants for the Reactions of Free Radicals with Oxygen in Solution. *J. Am. Chem. Soc.* **1983**, *105*, 5095–5099.
- (18) Serpone, N.; Salinaro, A. Terminology, Relative Photonic Efficiencies and Quantum Yields in Heterogeneous Photocatalysis. Part 1: Suggested Protocol. *Pure Appl. Chem.* **1999**, *71*, 303–320.
- (19) (a) Hatchard, C. G.; Parker, C. A. A New Sensitive Chemical Actinometer – II. Potassium Ferrioxalate as a Standard Chemical Actinometer. *Proc. R. Soc. London, Ser. A* **1956**, *235*, 518–536. (b) Su, R.; Dimitratos, N.; Liu, J.; Carter, E.; Althahban, S.; Wang, X.; Shen,

Y.; Wendt, S.; Wen, X.; Niemantsverdriet, J. W.; Iversen, B. B.; Kiely, C. J.; Hutchings, G. J.; Besenbacher, F. Mechanistic Insight into the Interaction Between a Titanium Dioxide Photocatalyst and PdI Cocatalyst for Improved Photocatalytic Performance. *ACS Catal.* **2016**, *6*, 4239–4247.

(20) (a) Kraeutler, B.; Bard, A. J. Heterogeneous Photocatalytic Synthesis of Methane from Acetic Acid – new Kolbe Reaction Pathway. *J. Am. Chem. Soc.* **1978**, *100*, 2239–2240. (b) Kraeutler, B.; Bard, A. J. Photoelectrosynthesis of Ethane From Acetate Ion at an N-Type Titanium Dioxide Electrode. The Photo-Kolbe Reaction. *J. Am. Chem. Soc.* **1977**, *99*, 7729–7731.

(21) Oliver, E. W.; Evans, D. H. Electrochemical Studies of Six N-F Electrophilic Fluorinating Reagents. *J. Electroanal. Chem.* **1999**, *474*, 1–8.

(22) Lantaño, B.; Postigo, L. Radical Fluorination Reactions by Thermal and Photoinduced Methods. *Org. Biomol. Chem.* **2017**, *15*, 9954–9973.